Title
THERMOGRAVIMETRIC ANALYSIS OF IRON-SODIUM SILICATE REACTIONS

Author
Wada, K.R.

Publication Date
1983-06-01

Lawrence Berkeley Laboratory
UNIVERSITY OF CALIFORNIA

Materials & Molecular Research Division

THERMOGRAVIMETRIC ANALYSIS OF IRON-SODIUM SILICATE REACTIONS

K.R. Wada
(M.S. Thesis)

June 1983

Prepared for the U.S. Department of Energy under Contract DE-AC03-76SF00098

DISCLAIMER

LBL-15599

THERMOGRAVIMETRIC ANALYSIS OF IRON SODIUM SILICATE REACTIONS

Kenneth Wada

(M.S. Thesis)

University of California
Lawrence Berkeley Laboratory
Berkeley, CA 94720

This work was supported by the Director, Office of Energy Research, Office of Basic Energy Sciences, Materials Sciences Division of the U. S. Department of Energy under Contract No. DE-AC03-76SF00098.

THERMAGRAVIMETRIC ANALYSIS OF IRON SODIUM SILICATE REACTIONS

Kenneth Wada

University of California
Lawrence Berkeley Laboratory
Berkeley, CA 94720

June, 1983

ABSTRACT

Sodium disilicate glass will react with pure iron at elevated temperatures and reduced pressures to form sodium gas, iron(II) oxide, and iron(III) oxide as the major products. This reaction is shown to be sensitive to the previous history of the iron specimen. That is, if the iron substrate is characterized by a high activity of oxygen, the reaction to form sodium gas will be hindered. In this study the decomposition kinetics of the glass on the iron substrate were investigated using various quantitative kinetic models and data generated by thermogravimetric analysis.

TABLE OF CONTENTS

Introduction. 1

Theoretical 3

Thermodynamics of the Proposed Reaction Sequence. 5

Reaction Rate Theory. 6

Mass Transfer Considerations. 9

Heterogeneous Reactions 12

Experimental. 15

Materials 15

Experimental Apparatus. 16

Experimental Procedure. 18

Results and Discussion. 20

Conclusions 26

References. 28

Acknowledgements. 30

Appendix A. 31

Introduction

A current theory of glass-to-metal bonding requires interface saturation with the lowest valence metal oxide for chemical bonding to occur. The interface is considered to be saturated when thermodynamic equilibrium exists between the glass and metal phases, or when the thermodynamic activity of the lowest valence metal oxide in the interfacial region is equal to unity. These concepts for the requirement of adherence of a glass to metal, have been developed from wetting and reaction studies of sodium silicate glasses on various metals.[1-5]

In most glass-metal systems, chemical reactions will occur once an intimate interface has formed. The reactions will continue until the system attains chemical thermodynamic equilibrium. Thus, it becomes important, in a scientific and engineering sense, to study the nature of the reactions and their rate of approach toward equilibrium. This is because the chemical reactions involved can maintain, lead to, or lead away from, the saturation of the interfacial zone with the lowest valence oxide of the substrate metal.

The manner in which interfacial reactions proceed in a glass-metal system and the nature of the reaction sequences, has been studied for sodium silicate glass-metal systems involving iron,[2,4-6,8], iron-cobalt alloys,[4,7] and platinum,[3] to name a few. These studies were generally qualitative or semiquantitative in nature, and established a basis for understanding the reactions which occur in a glass-metal system.

Generally, the reactions that are known to occur near the interface involve a change in the valence of the reaction species. These reactions (redox reactions) play an important role in the rate of chemical change near the interface for a glass-metal system. Thus, understanding the nature of the reaction sequences, the speed or kinetics, and how certain parameters, such as temperature, and sample history affect the reactions should give further insight into the interplay of the redox reactions governing the development of the glass-metal interface.

Factors that can have an important influence on the kinetics of a glass-metal redox reaction are mass-transfer effects such as the dissolution of metal oxide into the molten glass. Most kinetic models in heterogeneous reaction systems usually take mass transfer and interfacial kinetics into account.

As yet, no known systems have been investigated in a complete, quantitative fashion. It will be the purpose of this work to establish a quantitative model describing the reactions and mass transport phenomena involved in a typical glass-metal system.

Theoretical

Extensive work on the iron-sodium disilicate system has been done.[2-8] Also, thermodynamic data for this system is readily available.[9-10] However, an extensive literature search has yielded no quantitative studies of the iron-sodium disilicate system. There are two semi-quantitative studies done on this system,[4-6] with the rest being qualitative in nature. With these considerations in mind, the iron-sodium disilicate reactions will make an ideal case study for a systematic quantitative analysis of the reaction kinetics of a glass-metal system.

The modeling approach will consist of describing the possible reaction steps that may take place within the system. The plausibility of the proposed reaction sequence will be checked using thermodynamic data that is available from the literature. Once the reaction sequence has been established, a chemical rate theory will be applied to the proposed reaction system. This process should give the integrated rate equation that describes the chemical rate process under study.

The mass transfer effects will be considered next, and the diffusion-limited rate equation shall be derived. However, in some reactions, especially those with heterogeneous phases, both diffusion and interfacial reactions must be included. Thus, a third case will deal with the combined effects of diffusion and reaction. The resulting models will then be tested for validity, and if possible, the temperature dependence of the interfacial reactions will be determined.

Using thermogravimetric and sessile drop measurements, Tomsia and Pask have proposed the following reaction scheme for the iron-sodium silicate system.[6] The primary reaction, when no wustite is present in the glass, is the reduction of soda in the glass by iron to form iron (I) oxide and sodium gas.

$$Fe(s) + Na_2O(int) \xrightarrow{k_1} FeO(int) + 2Na(g)\uparrow \quad (1)$$

The iron oxide formed at the interface, subsequently diffuses into the glass where it can undergo further oxidation to form ferric oxide.

$$FeO(int) = FeO(glass) \quad (2)$$

$$2FeO(glass) + Na_2O(glass) \xrightarrow{k_2} Fe_2O_3(glass) + 2Na(g)\uparrow \quad (3)$$

Reaction (3) is followed by the diffusion of ferric oxide from the glass to the glass-metal interface.

$$Fe_2O_3(glass) = Fe_2O_3(int). \quad (4)$$

The ferric oxide at the glass-metal interface can undergo a reduction reaction to form more ferrous oxide via the following process:

$$Fe(s) + Fe_2O_3(int) \xrightarrow{k_3} 3FeO(int). \quad (5)$$

Notice, that in describing the reactions, the following were used:

s = Iron in the solid phase, at the interface.

int = Interface at glass-metal junction.

g = Gas phase.

k_1 = Irreversible reaction rate constant for reaction (1)

k_2 = Irreversible reaction rate constant for reaction (3)

k_3 = Irreversible reaction rate constant for reaction (5)

The production of ferrous ions via reaction (5) will contribute to the production of sodium gas via reaction (3). Thus, if the sequence proposed by Tomsia and Pask is valid, a reaction between sodium silicate glass doped with FeO, and iron metal should result in a higher amount of weight loss than that for a homogeneous reaction of FeO in the glass with soda in the glass.

Thermodynamics of the Proposed Reaction Sequence

The change in free energies for reactions (1) and (3), in a closed, constant temperature, and constant pressure system are:

$$\Delta G_T = \Delta G_T^\circ + RT \ln \frac{a_{FeO_{(int)}} \quad (P)^2_{Na}}{a_{Na_2O_{(gl)}} \quad a_{Fe(s)}} \qquad (6)$$

and,

$$\Delta G_T = \Delta G_T^\circ + RT \ln \frac{a_{Fe_2O_{3(gl)}} \quad (P)^2_{Na}}{a_{Na_2O_{(gl)}} \quad a^2_{FeO_{(gl)}}} \quad , \qquad (7)$$

The standard free energies at 1000°C, for (1) and (3) were calculated to be 291 kJ/mole, and 328 kJ/mole respectively.[11] The equilibrium pressure of the sodium gas for reaction (1) at 1000°C, (assuming $a_{Fe} = 1$ and $a(FeO)/a(Na_2O) \leq 1$) is greater than or equal to 0.1096 Pa. Also, the equilibrium pressure of the sodium gas for reaction (3), (in this case the ratio of the activities will probably be less than or equal to one)* will be approximately equal to 0.0193 Pa.

---

* This assumes that some soda is present in the glass, and that $a(Fe_2O_3)/a(FeO) \leq 1$.

Thus, reactions (1) and (3) should proceed, if the total ambient pressure is less than .01 Pa, until an equilibrium concentration of ferric to ferrous ions is attained in the glass. The standard free energy at 1000°C for reaction (5) is negative, -50.6 kJ/mole. Thus, there are no thermodynamic barriers towards product formation in reactions (1), (3) and (5) at 1000°C. Even though thermodynamics tells us that the reactions should proceed spontaneously, this does not give any information regarding the reaction kinetics. Thus, the kinetics must be derived in some fashion from what we know of the proposed elementary reaction scheme.

Reaction Rate Theory

The reaction rate for complex reactions and all elementary reactions has the following phenomenological concentration dependence:

$$R_j = k_j \prod_{i=1}^{n} C_i^{|\nu_{ij}|} \tag{8}$$

where:

R_j = Rate of jth reaction process.

k_j = Reaction rate constant for the jth process.

n = Number of components participating in the jth reaction.

C_i = Concentration of the i_{th} component.

ν_{ij} = Stoichiometric coefficient for component i in reaction j
is positive if the i_{th} component is a product and
is negative if the i_{th} component is a reactant.

The rate of production or consumption of component i, in the j_{th} reaction sequence has the following form:

$$r_{ij} = \nu_{ij} R_j \tag{9}$$

The overall production or consumption of a component species will be the sum of all reaction sequences where the ith component takes part, or for a complex reaction sequence:

$$r_i = \sum_{j=1}^{N} \nu_{ij} R_j \quad . \tag{10}$$

where N is the number of elementary, or step reactions.

Using the rate laws for elementary reactions given above, the rate of consumption of sodium ions in the glass can be given as:

$$r_{Na_2O} = - k_1 \left[Na_2O_{(int)}\right] - k_2\left[FeO_{(gl)}\right]^2 \left[Na_2O_{(gl)}\right] \tag{11}$$

where the brackets denote concentration. If we can assume reactions (3) and (5) to proceed appreciably faster than (1), then reaction (1) will become the dominant rate-controlling step. Using this assumption, we can invoke what is known in physical chemistry as the Quasi-Steady-State-Assumption, or QSSA.

The QSSA states that if the intermediates are being produced and consumed rapidly, then the over-all contributions of the rate of production of the intermediates will be equal to zero. Or in other words, the intermediates will form rapidly in the system till a steady-state concentration is achieved. This can be stated as:

$$r_{FeO} = \frac{d\left[FeO_{(gl)}\right]}{dt} = 0 \tag{12}$$

for the total FeO production rate during steady state. For the FeO production rate, during steady state:

$$r_{FeO} = \frac{d[FeO_{(gl)}]}{dt} = 0 = - k_2[FeO_{(gl)}]^2[Na_2O_{(gl)}] \tag{13}$$

yields the following result for the rate of soda consumption:

$$r_{Na_2O} = - k_1 [Na_2O_{(int)}] \qquad (14)$$

For all preceeding equations, the cation concentrations are expressed in terms of oxide concentrations. This is due to the fact that electroneutrality must be achieved in the system by balancing the cations with the oxygen anions.

If the rate of sodium ion consumption is dominated by the interfacial reaction, the rate of consumption should be linearly proportional to the amount of soda present near the interface. If we integrate equation (14) and note that, by stoichiometry, two sodium atoms are liberated for every soda molecule, the following integrated rate equation describing the kinetics of the sodium weight loss is obtained:

$$1 - \frac{N'}{N_I} = \exp(-KAt) \qquad (15)$$

where:

N_I = Number of sodium equivalents initially in the glass.

N' = Amount of sodium liberated from the glass.

A = Interfacial surface area.

K = Interface reaction constant.

t = Time of reaction.

The important result one obtains from (15) is that a semi-log plot of left-hand-side of (15) vs. the time, t, should result in a straight line, with the slope being equal to the reaction rate constant times the interfacial area.

Mass Transfer Considerations

For many solid-state reactions, the mass transfer rate of the reactants governs the reaction rate. This assumes that the reaction proceeds at an infinitely fast rate. Reactions that fit this category, are called mass transport limited.

If the iron-sodium silicate reactions are mass-transport limited, and assuming that convection can be neglected as one of the contributions to mass transfer of the reactants to the interface,* then the system can be modeled using flux contributions due to diffusion of the reactants in the bulk glass media. For the geometry shown in Fig. 1, one can use the one-dimensional form of the diffusion equations; also known as Fick's 1st and 2nd laws of diffusion in one dimension, for isotropic media, or:**

$$J_i = -D_i \frac{\partial C_i}{\partial x} \tag{16}$$

and

$$\frac{\partial C_i}{\partial t} = \frac{\partial}{\partial x} \left\{ D_i \frac{\partial C_i}{\partial x} \right\} \tag{17}$$

---

* There are no density gradients contributing to natural or free convection in the glass. Also the system is static, i.e., there is no hydrodynamic flow of the glass on the metal substrate.

* Borom and Pask have shown that eq. (16) is applicable in this system. This is because the diffusivity is independent of concentration.

where

J_i = Flux of component i in the glass.

C_i = Concentration of component i in the glass.

D_i = The effective binary diffusion coefficient of species i, in the glass.

Borom and Pask (12) have determined the effective binary diffusion coefficients for the chemical species in the iron-sodium silicate system, and have shown the chemical interdiffusivity of soda in the glass to be essentially concentration independent within the temperature and composition ranges incorporated in this study.

Noting the geometry shown in Fig. 1, the glass layer of thickness ℓ covers the metal. The direction perpendicular to the glass-metal interface is considered to be the x-direction. The interface is located at $x = 0$, and the glass surface is located at $x = \ell$. The metal substrate is assumed to extend to $x \to -\infty$. Also, for simplification of the diffusion equations, the interface is considered to be stationary with respect to the glass surface.

Using the assumptions and geometry described above, the following boundary conditions can be applied: First, at $x = 0$, assuming the interfacial reaction to be infinitely fast, the concentration is fixed, or;

$$C_{Na_2O} \Big/_{x = 0} = C_o \cdot \qquad (18)$$

where C_o is the final equilibrium concentration of the soda in the glass.

Second, at $x = \ell$, and adding the assumption that the evaporation of the soda on the glass surface is very small, the flux of soda at $x = \ell$ is zero, or:

$$J_{Na_2O}\Big/_{x = \ell} = 0 \tag{19}$$

or

$$\frac{\partial C}{\partial x}(Na_2O)\Big/_{x = \ell} = 0 \quad . \tag{20}$$

The initial condition requires the glass to have a uniform concentration of soda in the glass.

Application of the boundary conditions, and the initial conditions to the differential equation given in (17) gives the following result for the sodium weight loss (Appendix A).

$$M_t = M_w N_I \left\{1 - \frac{8}{\pi^2} \sum_{m=0}^{\infty} \frac{\exp[-(2m+1)^2 \pi^2 t'/4]}{(2m+1)^2}\right\} \tag{21}$$

where:

M_t = Sodium weight loss in grams.

M_w = Molecular weight of Na (grams/g-mole).

N^I = Equivalents of sodium in the glass.

t' = Dimensionless time = $\ell^2 t/D$.

Note that for the case where ℓ approaches infinity, it will give a parabolic rate law for the loss of soda in the glass, or

$$M_t^2 = K_p t \tag{22}$$

K_p = parabolic rate constant.

Heterogeneous Reactions

Now, we come to the third, and final case that deserves some attention. The case in question, involves the coupling of kinetic phenomena, that is, the coupling of mass transfer rates with reaction rates to give the overall result. This class of reactions frequently occurs in solid-fluid systems, and can only be dealt with on a case-by-case basis.[13,14] The advantage of this method of approach is realized by giving a more complete analysis of the reaction rates. The more complete analysis is beneficial, because if interpreted properly, it can give valuable insight to the reduction reaction at the glass-metal interface. The chief disadvantage lies in the inherent complexity of the analysis.

For coupled reactions in heterogeneous systems, the boundary conditions given in (18) no longer apply. The new boundary condition at $x = 0$, states that the concentration of the soda at the interface is not quite zero, but a rapidly decreasing function with respect to time. The function can be determined by integrating (14) for the concentration of soda at the interface, and assuming reactions (3) and (5) to occur much faster than reaction (1). In mathematical terms:

$$C_{Na_2O}\Big|_{INT} = C_{Na_2O(I)}\, e^{-KAt} \,. \tag{23}$$

The boundary condition at $x = \ell$, and the initial condition do not change. The new boundary condition makes the solution of the diffusion equation much more complex in nature, and the method of Laplace transform analysis must be utilized in order to attain a solution. The resulting solution is (18):

$$M_t = N_I M_w \left\{ 1 - \exp(-KAt) \quad \left(\frac{D}{KA\ell^2}\right)^{1/2} \tan(KA\ell^2/D)^{1/2} \right\}$$

$$- \frac{8}{\pi^2} \sum_{n=0}^{\infty} \frac{\exp \quad (2n+1)^2 \pi^2 Dt/4\ell^2}{(2n+1)^2 \left[1 - (2n+1)^2 \pi^2 / 4(KA\ell^2/D)\right]} \quad . \qquad (24)$$

Notice that equation (24) shows the importance of the dimensionless parameter $KA\ell^2/D$. If the reaction rate is very large, then (24) will decompose after some manipulation, to equation (20); the reaction is said to be "diffusion controlled". The same will hold true if the diffusivity is much smaller than the reaction rate constant times the surface area. On the other hand, if the reaction rate constant and the surface area are much smaller than the diffusivity, then equation (24) will become that for the reaction limited case.

Obtaining the experimental values for the reaction rate constants as a function of time and temperature would be quite tedious by using (24). If the reaction rate were indeed small, then the nonlinear boundary condition (23) can be expanded in a Taylor's series, and the resultant nonlinear terms could be dropped out. Also if the ratio of $KA\ell^2/D$ is much less than unity, so that one could consider the geometry to be a semi-infinite couple, then the following equation would result (Appendix A), (again using the method of Laplace Transforms).

$$\frac{M_t}{A} = \frac{\rho KA\sqrt{D}(8000)M_{w(Na)}}{3\, M_{w(glass)}\sqrt{\pi}}\, t^{3/2} \quad . \qquad (25)$$

where:

$M_{w(Na)}$ = Molecular wt. of sodium.

ρ = Initial density of the glass at temperature.

M_w(glass) = Molecular wt. of glass.

t = Time (seconds).

Equation (25) shows an important result, in that, if the log of the weight loss per area were plotted against the log of the time, a straight line would result, with a slope of 1.5. Knowing the material parameters, and the intercept will yield a usable value for the reaction rate constant.

Experimental

Materials

Substrates of Marz A iron(*), in the form of 0.254mm thick foils were used. The iron was specified to be 99.995 wt % pure. The major impurities were carbon (.002 wt %) and oxygen (.003 wt %). Before each experimental run, the Marz A iron was annealled in a graphite furnace at 1100°C for 18 hours. Armco iron was obtained in the form of a 1mm thick sheet, of reported 99.8 percent purity, with a typical analysis of 0.015 wt % carbon, 0.025 wt % manganese, 0.005 wt % phosphorus, 0.025 wt % sulphur, and 0.002 wt % silicon. Precipitates of FeO were detected metallographically. Rectangular specimens were cut to provide surface areas of approximately 0.5 to 1.00 square centimeters. All specimens were polished with dry 400 mesh SiC paper, and given a final metallurgical polish on a lap wheel with 0.05 micron alumina. The samples were cleaned in ethyl alcohol, acetone and distilled water in an ultrasonic cleaner. All samples were prepared immediately prior to the experiment.

Sodium disilicate glass (NS_2) was prepared using reagent-grade sodium carbonate and fused silica glass(**). Batch materials to yield 0.25 kilograms of glass were mixed with isopropyl alcohol for 24 hours, slowly dried at 60°C, melted at 1350°C in air for 3 hours with occasional stirring in a platinum crucible; and subsequently were cooled and crushed. The glass was melted twice to insure homogeneity.

---

* MRC., Orangeburg, N. Y.
** 7940, 325 mesh, Corning Glass Works, Corning, N. Y.

The final melt was outgassed at 1200°C for 2 hours.* The glass was cut with a diamond saw under kerosene, into cubes with a nominal edge size of 2.0mm, and stored in a vacuum desiccator until used. The chemical composition of NS_2 and other glasses used in this study are presented in Table 1.

Experimental Apparatus

The furnace consisted of a Kanthal wire-wound, high density (Coors AD-998) alumina tube (2.0 cm in diameter by 53 cm long), (Fig. 2). The hot zone is approximately 30.4 cm long, and the wire was wound to provide a flat < 2°C/cm temperature gradient inside the tube. Both ends of the furnace were sealed with water-cooled Viton o-rings. The temperature inside the furnace was measured with a Pt-Pt10Rh thermocouple to ± 1°C. The temperature measurements were calibrated electronically within the 355° to 1200°C range with a precision microvolt potentiometer attached to a standard reference thermocouple. 100 mg of calcium carbonate was decomposed and checked against the decomposition temperature found in the literature.[11] The accuracy of the temperature measurement and control was found to be within 2°C.

A Cahn R-100 automatic, precision microbalance was attached to the furnace, and differential weight measurements were obtained with respect to time. The balance was calibrated against 10 mg and 100 mg standard weights and adjusted electronically to within 10 micrograms.

---

* This is the time and temperature required before bubbling of the glass completely ceases.

Table 1. Chemical Analyses of Glasses

Oxide constituent	Amount present in glass (wt %)	
	NS2 (wt %)	Glass + 40 wt FeO
SiO_2	64.38	38.63
Na_2O	33.85	20.31
FeO	0.00	38.23
Fe_2O_3	0.00	2.15
Al_2O_3	0.63	.38
TiO_2	0.001	.001
CaO	0.13	.078
MgO	0.02	.012
K_2O	0.05	.030
B_2O_3	0.18	.108

Continuous weight loss measurements were recorded on a strip chart recorder to within ± 0.1 percent accuracy on a 10.00 mg full scale. Weight measurements taken before and after each experiment showed errors of no greater than 10 micrograms.

The entire system, including the balance was sealed and subjected to a 6.67×10^{-3} Pa vacuum. The vacuum was produced by a liquid-nitrogen cold-trapped oil diffusion pump. The pressure was measured with a calibrated, cold-cathode ionization gauge.

Experimental Procedure

The reactions were carried out at temperatures over the interval, 955°C to 1145°C in 6.67×10^{-3} Pa vacuum. The loss in weight was initially recorded in milligrams on the strip-chart recorder. The weight loss was then converted to the fractional sodium lost from the glass by redox reactions. The amount of sodium weight loss per square centimeter of interfacial area was also calculated and recorded.*

The procedure for a test consisted of pumping the system down to approximately 0.10 Pa, then closing all vacuum valves while ultra-pure helium was admitted to atmospheric pressure. The system was pumped down again, to approximately 0.10 Pa. Afterwards, a liquid nitrogen-trapped diffusion pump reduced the pressure to the working (6.67×10^{-3} Pa) value.

---

* The glass completely wets the surface of the metal above 900°C within one minute.

After maintaining the vacuum for 20 minutes, the balance was tared and zeroed using an external precision resistor network. The furnace was heated from room temperature to the softening point of the glass (840°C), at 20°C/minute. The specimen was held at 840°C under vacuum for one hour. The furnace was heated again to the working temperature at approximately 100°C per minute so that the experiment could be held under almost isothermal conditions. When the final temperature was attained, the test was carried out, and the furnace cooled at the end of the experiment to room temperature.

The above procedures were followed for all Marz-A iron experiments with NS2. One run each with Armco iron, aged Marz-A iron (7 months aging in a vacuum desiccator), and fused silica (blank run) as substrates were also done. Sodium disilicate glass doped with 40 wt % FeO were placed on Armco iron and fused silica as substrates, and one run of each was done at 1030°C.

Results and Discussion

Figure 3, shows the experimental data for as-received Marz-A iron specimens obtained at four different temperatures. The data is plotted as a normalized weight loss, with respect to the equivalent sodium ions. The curves for the data are generally sigmoidal in shape. That is, there is a slow initial rate, followed by a faster reaction after approximately 30 minutes. Then, the rate tapers off at longer times.

Inspection of Fig. 4, shows the reaction behavior of FeO-doped glass on two different substrates. The top curve is for Armco iron as the substrate, and the bottom one is for a fused-silica substrate. The increase in reactivity shown with Armco iron can be explained by the reaction sequence (3) through (5). That is, in the presence of iron, iron(II) oxide can be formed by the reaction between the iron(III) and iron(0) species at the interface of the glass/metal junction. And, the presence of more iron(II) oxide, will drive reaction (3) further to form more products. Since no 'free' iron is present in the fused-silica experiment, we observe a reduction in the reaction, as shown in Fig. 4.

Figures 5 and 6 show attempts to linearize the kinetics of Fig. 3 using equation (15). The curves are not very linear for the high temperature reactions, (Figs. 5A, 5B and 6A). But the lower temperature, Fig. 6B, shows a tendency for the reaction to dominate the over-all kinetic of soda decomposition.

Figures 7a and 7b show further attempts to linearize the data, assuming a semi-infinite couple, with diffusion being the predominant

mechanism. Again, the approach to linearity is quite poor. These results suggest that for the iron-sodium silicate system, the reactions tend to be dominated by the interfacial reaction, with some modifications to the overall scheme by mass-transport, and bulk reactions, (i.e., reaction sequences 3 to 5).

The above attempts to undertake a simplistic linearization scheme clearly shows that we are not considering the entire picture of the reactions. We must also consider mass transfer effects in a detail necessary to affect a solution towards understanding the interplay of reactions with transport phenomena, that contribute to the observed behavior. Thus, the next step would be to add one more degree of complexity, and if possible to further add descriptive models to the system. Taking the aforementioned arguments into account, and noticing that equation (25) can be readily linearized on a log-log plot, we obtain Fig. 8. Inspection of this figure shows very nearly linear plots over a period of times. A linear regression analysis (up to 90 percent reaction) gives very good correlations, (with regression coefficients of 0.997 or better). The equations for the lines for the three higher temperatures are given in Table 2. The kinetic data for the low (955°C) temperature reaction was obtained from Fig. 5B.

The kinetic parameters for the 1146°C reaction were substituted into equation (24), and compared with the experimental data. The result of this calculation is shown in Fig. 9. The theoretical model for the heterogeneous reaction system derived earlier works quite well within experimental error, up to one hour. After the reaction proceeds to the one hour time limit, a noticeable deviation begins to occur.

Table 2. Kinetic Data for the Iron-Sodium Silicate System

Temp..	Area	Diff.	Slope	Int.	Rate Const.
1228	0.6888	3.0×10^{-7}	----	---	4.83×10^{-6}
1303	0.4195	6.5×10^{-7}	1.51	5.56×10^{-6}	3.36×10^{-5}
1319	0.6703	7.5×10^{-7}	1.50	2.17×10^{-5}	7.66×10^{-5}
1419	0.4623	2.0×10^{-6}	1.40	4.71×10^{-4}	1.47×10^{-3}

Temp. = Temperature in Kelvin.

Area = Interfacial area in square centimeters.

Diff. = Diffusivity in cgs units. (From reference 12).

Slope = Slope of log-log plot.

Int. = Intercept of log-log plot (mass per interfacial area).

Rate constant is derived from the intercept, (units of inverse square centimeters per second).

That is, the data shows a reduction in the sodium weight loss as compared with the theory. This result can be rationalized if one looks at the phase diagram for the soda-silica-wustite system (Fig. 10). The reaction path is shown by the the line connecting point A to B. As one goes from pure sodium disilicate, to a mixture containing iron oxide, a phase change will occur at the 1110°C isotherm. The phase to be precipitated is cristobalite. The position on the diagram where this effect takes place is roughly equal to a sodium weight loss of about 60 wt %, with respect to equivalent sodium ions. Notice that the assumption is being made here that the presence of iron(III) oxide should not alter the effect of the silica precipitation reaction. Further evidence of the precipitates being formed, can be readily seen in Fig. 11. The precipitates have been shown, by Kevex analysis to be silicon rich. Considering the aforementioned observations, it would seem likely that the precipitates will hinder the transport of the reactant sodium ions from the bulk glass to the interfacial region, thereby resulting in the observed decrease in the rate not predicted by the theory.

The exact fits for the lower temperatures were not as good as seen in Fig. 9. However, for short times, in all cases, the fit was nearly perfect. The observed trends can be summarized in this case by the theoretical model predictions of too low a weight loss after short times. This could be due to the failure of the geometrical assumption of a semi-infinite couple used to derive the kinetic parameters; but a more plausible argument can be found by dismantling the Q.S.S.A. The Q.S.S.A. implies that the entire reaction sequence occurs at, or near

the interface. This assumption will not hold if any appreciable bulk glass reaction can occur. That is, if the diffusion of ferric oxide is relatively slow, one can expect reaction (3) to play a more important effect in the overall kinetics of the bulk glass reaction, thus changing the differential equations, and resulting in a nonlinear higher order partial differential equation that would not be amenable to an analytical solution. However, for the high temperature case, the 3-5 reaction sequence could be occurring rapidly enough to make the implied interfacial boundary condition (equation 22) hold.

The temperature dependence of the reaction rate constant is represented by the well known Arrhenius equation.

$$k = k'e^{-Ea/RT} \tag{26}$$

where k' is the pre-exponential factor, E_a the activation energy of the interfacial reaction, and R is the universal gas constant. Thus plotting the log of the rate constant versus the reciprocal temperature in degrees Kelvin, should result in a straight-line plot. The results of this type of plot, for the iron-sodium disilicate reaction system, yields the curve shown in Fig. 12. The calculated value for the activation energy is 463 kJ per mole, and the pre-exponential factor is 9.53×10^{13} $cm^{-2}s^{-1}$.

The effects of sample history were also studied, and the results are shown in Figs. 12 and 13. Figure 12 shows an interesting case where aging can play a significant role in the reduction of the reaction rate constant. This result has also been found by others in this lab (6). Assuming that the initiation reaction is the slow step (reaction 1), if we change the thermodynamic driving force of

reaction 1, to favor the reactants, then we should observe some reduction in the reactivity of the metal. A thermochemical balance of the Gibbs free energies given in equation 6, shows that a high activity of FeO at the interface can shift the driving forces for chemical reaction towards the reactants. The aged Marz-A iron was subjected to an Auger analyses for the oxygen content, and was found to be saturated with oxygen, thus giving credence to the argument mentioned above. Figure 14 shows a similar effect. That is, the reduction of reactivity in Armco iron. However, one should note, that an increased activity of the iron(I) oxide in the bulk glass phase will not necessarily reduce the glass-metal redox reaction. But in effect, a high bulk activity, due to sequence 3-5 will enhance the reduction of the sodium ions in the glass

Conclusions

For most heterogeneous reactions, the mode is usually quite complex in nature. This is chiefly due to the fact that mass transport and interfacial reactions can be coupled in some instances, as it was for the iron-sodium disilicate reactions. The coupling will usually occur when the flux contributions due to the mass transport, and reactions are not negligible with respect to each other. This is particularly true for solid-liquid systems, where the surface reaction is slow.[13]

Analyses of heterogeneous reactions almost always utilize the methodology of mass balances with generation effects. Also, if convectional transport is to be taken into account, a momentum balance must also be accounted for. Even so, the modeling of each system should follow a case-by-case basis of approach. The importance of proceeding in this fashion is that it will help one to deal with coupling of the side reactions with the main elementary reactions and mass transport. Even though this coupling can and will almost always lead to nonlinearities in the model, which are not amenable to a direct analysis or calculation, the model can tell us when and how significantly the side reactions can perturb the system in question. Also, we can gain further insight as to which parameters enhance or reduce these reactions, which may be useful from an engineering point-of-view.

The importance of the difference between bulk activities, and interfacial values for the activities can be shown in an indirect manner by measuring the reactivities with respect to changes in the

activities of the reacting species. Analyzing the reaction kinetics for a glass-metal interaction, although complex, can help us to understand more about the development of the interface, and also helps us to better appreciate the connections between equilibrium concepts and reaction dynamics.

References

1. J. A. Pask and R. M. Fulrath, "Fundamentals of Glass-to-Metal Bonding: VIII, Nature of Wetting and Adherence," J. Am. Ceram. Soc. 45 [12] 592-596 (1962).
2. F. D. Gaidos and J. A. Pask, "Effect of Glass Composition on the Glass-Iron Interface," in Advances in Glass Technology (Plenum Press, New York, 1962), pp. 548-565.
3. J. J. Brennan and J. A. Pask, "Effect of Composition on Glass Metal Interface Reactions and Adherence," J. Am. Ceram. Soc. 56 [2] 58-62 (1973).
4. M. P. Borom, J. A. Longwell, and J. A. Pask, "Reactions Between Metallic Iron and Cobalt Oxide Bearing Sodium Disilicate Glass," J. Am. Ceram. Soc. 50 [2] 61-66 (1967).
5. J. J. Brennan, "The Affect of Atmosphere and Glass Composition on Reactions at Glass-Metal Interfaces," Lawrence Radiation Laboratory Report UCRL-19045 (1969).
6. A. P. Tomsia and J. A. Pask, "Kinetics of Iron-Sodium Disilicate Reactions and Wetting," J. Am. Ceram. Soc. 64 [9] 523-528 (1981).
7. J. A. Pask and A. P. Tomsia, "Wetting, Spreading and Reactions at Liquid/Solid Interfaces," in Surfaces and Interfaces in Ceramic and Ceramic-Metal Systems, J. A. Pask and A. G. Evans ed., (Plenum Press, New York 1981), pp 411-419.
8. L. G. Hagen and S. F. Ravitz, "Fundamentals of Glass-to-Metal Bonding: VI Reaction Between Metallic Iron and Molten Sodium Disilicate," J. Am. Ceram. Soc., 44 pp. 428-429, (1969).

9. P. T. Carter and M. Ibrahim, "Ternary System Na_2O-FeO-SiO_2," J. Soc. Glass Technol., 36 [170] 142-63T (1952).

10. A. M. Lacy and J. A. Pask, "Electrochemical Studies in Glass: II," J. Am. Ceram. Soc., 53 [12] 676-79 (1970).

11. JANAF Thermochemical Data, The Dow Chemical Company, Thermal Research Laboratory, Midland, Mich., Sept. 30, 1967.

12. R. E. Weston and H. A. Schwarz, Chemical Kinetics, (Prentice Hall, Englewood Cliffs, New Jersey 1972).

13. Handbook of Chemistry and Physics, 61 edition, (1981).

14. M. Borom and J. A. Pask, "Kinetics of Dissolution and Diffusion of the Oxides of Iron in Sodium Disilicate Glass," J. Am. Ceram. Soc. 51 [9], 490-498 (1968).

15. Bird, Stewart and Lightfoot, Transport Phenomena, (John Wiley, New York, 1960).

16. Chemical Engineers Handbook, 5th ed. (McGraw-Hill, New York, 1973).

17. C. R. Wylie, Advanced Engineering Mathematics, 4th ed. (McGraw-Hill, New York, N.Y., 1975).

18. J. Crank, The Mathematics of Diffusion, 2nd. (Oxford University Press, Oxford, Great Britain, 1975).

ACKNOWLEDGEMENTS

This work was made possible from grants provided by the National Institute of Health and the American Dental Association. The author also wishes to thank Dr. Pask for many discussions concerning this work. Also, the author wishes to thank Dr. Tomsia for preparing most of the raw materials and doing the characterizations on this system. Last, but not least of all, many thanks go to my wife Laura and my family, for their constant support throughout the writing of this document.

APPENDIX A

Derivation of equation (21)

First, we start with equation (17) and assume that the chemical interdiffusivity of the soda in the glass is independent with respect to the concentration of the soda in the glass.

$$D \frac{\partial C^2}{\partial x^2} = \frac{\partial C}{\partial t} \tag{A1}$$

where C is the soda concentration and D is the chemical interdiffusivity of the soda in the glass.[14]

The initial condition is:

$$C_{t=o} = C_I \tag{A2}$$

C_I is the initial soda concentration in the glass. The boundary condition at x = 0 is Co. Where Co is the final equilibrium concentration of the soda in the glass. The second boundary condition states that the flux of soda at x = ℓ is zero, or:

$$\left.\frac{\partial C}{\partial x}\right/_{x=\ell} = 0 \tag{A3}$$

If we made the units dimensionless, the following equation may be obtained:

$$\frac{\partial^2 C'}{\partial X^2} = \frac{\partial C'}{\partial t'} \tag{A4}$$

where

$$C' = \frac{C_I - C}{C_I - Co}$$

$$t' = \frac{Dt}{2}$$

$$X' = \frac{x}{}$$

The initial condition changes to:

$$C' \Big/_{t'=o} = 0 \qquad \text{(A5)}$$

The first boundary condition (at X = 0) is:

$$C'/X=o = 1 \qquad \text{(A6)}$$

The second boundary condition (at x=) is:

$$\frac{\partial C'}{\partial X} \Big/_{X=1} = 0 \qquad \text{(A7)}$$

The solution to (A4) may be found by the use of the Laplace transformations. If we Laplace transform (A4), the following equation will be obtained:

$$sg - C'(X,0) = \frac{d^2g}{dX^2}$$

or

$$\frac{d^2g}{dX^2} - sg + C'(X,0) = 0 \qquad \text{(A8)}$$

where:

$$g = \int_0^\infty e^{-st} C'(X,t)dt \qquad \text{(A9)}$$

or

$$g = \mathcal{L} C'(X,t) \qquad \text{(A10)}$$

Substituting the initial condition into (A8) gives:

$$\frac{d^2g}{dX^2} - sg = 0 \tag{A11}$$

The general nontrivial solution to (A11) is:

$$g = Ae^{-\sqrt{s}X} + Be^{\sqrt{s}X} \tag{A12}$$

The transforms of the boundary conditions are:

$$\mathcal{L}\left\{C' \Big/ X=1\right\} = g \Big/ X=0 = \frac{1}{s} \tag{A13}$$

and

$$\mathcal{L}\left\{\frac{\partial C'}{\partial X} \Big/ X=1\right\} = \frac{dg}{dx} \Big/ X=1 = 0 \tag{A14}$$

Substitution of (A13) and (A14) into (A12) will result in the following:

$$\frac{1}{s} = A + B \tag{A15}$$

$$0 = -Ae^{-\sqrt{s}} + Be^{\sqrt{s}} \tag{A16}$$

Application of Cramer's rule to (A15) and (A16) results in a solution for A and B:[17]

$$A = \frac{\begin{vmatrix} \frac{1}{s} & 1 \\ 0 & e^{\sqrt{s}} \end{vmatrix}}{\begin{vmatrix} 1 & 1 \\ -e^{-\sqrt{s}} & e^{\sqrt{s}} \end{vmatrix}} = \frac{\frac{1}{s}e^{\sqrt{s}}}{e^{\sqrt{s}} + e^{-\sqrt{s}}} \tag{A17}$$

$$B = \frac{\begin{vmatrix} 1 & \frac{1}{s} \\ -e^{-\sqrt{s}} & 0 \end{vmatrix}}{\begin{vmatrix} 1 & 1 \\ -e^{-\sqrt{s}} & e^{\sqrt{s}} \end{vmatrix}} = \frac{\frac{1}{s}e^{-\sqrt{s}}}{e^{\sqrt{s}} + e^{-\sqrt{s}}} \tag{A18}$$

Substitution of (A17) and (A18) into (A12) yields:

$$g = \frac{\frac{1}{s}\left\{ e^{\sqrt{s}}\, e^{-\sqrt{s}X} + e^{-\sqrt{s}}\, e^{\sqrt{s}X} \right.}{e^{\sqrt{s}} + e^{-\sqrt{s}}}$$

$$= \frac{\frac{1}{s}\cosh\left(\sqrt{s}(1-X)\right)}{\cosh\sqrt{s}} \qquad \text{(A19)}$$

Thus:

$$C' = {}^{-1}\{g\} = -1\left\{\frac{\frac{1}{s}\cosh(\sqrt{s}(1-X))}{\cosh\sqrt{s}}\right\} \qquad \text{(A20)}$$

Application of the residue therem to (A20) gives:

$$C' = 1 - \frac{4}{\pi}\sum_{m=0}^{\infty}\left\{\frac{e^{-(2m+1)^2\pi^2 t'/4}}{(2m+1)}\sin\left[\frac{(2m+1)\pi x}{2}\right]\right\} \qquad \text{(A21)}$$

In terms of C:

$$C = C_o + (C_I - C_o)\frac{4}{\pi}\sum_{m=0}^{\infty}\left\{\frac{e^{-(2m+1)^2\pi^2 t'/4}}{(2m+1)}\sin\left[\frac{(2m+1)\pi x}{2}\right]\right\} \qquad \text{(A22)}$$

For the iron-sodium silicate system, C_o is very small.[6] Thus, $C_o \approx 0$, therefore:

$$C = C_I\frac{4}{\pi}\sum_{m=0}^{\infty}\left\{\frac{e^{-(2m+1)^2\pi^2 t'/4}}{(2m+1)}\sin\left[\frac{(2m+1)\pi x}{2}\right]\right\} \qquad \text{(A23)}$$

Integrating (A23) over the thickness of the glass, and multiplying the result by a constant cross-sectional area results in an equation giving the amount of soda left in the glass with respect to the dimensionless time t'. That is:

$$N = A\, C_I\, \frac{8}{\pi^2}\sum_{m=0}^{\infty}\frac{e^{-(2m+1)^2\pi^2 t'/4}}{(2m+1)^2} \qquad \text{(A24)}$$

By stoichiometry:

$$N(\text{sodium}) = 2\left\{N(Na_2O,\text{initial}) - N(Na_2O,t')\right\} \tag{A25}$$

And:

$$M_t = N(\text{sodium})M_w \tag{A26}$$

Where M_w is the atomic weight of sodium. Substitution of (A25) and (A26) into (A24) gives a final rsult for M_t.

$$M_t = M_w N_I \left\{1 - \frac{8}{\pi^2}\sum_{m=0}^{\infty}\frac{\exp[-(2m+1)^2\pi^2 t'/4]}{(2m+1)^2}\right\} \tag{A27}$$

Note that $N_I = 2A\,C_I$, which is the gram equivalents of sodium initially in the glass.

Derivation of Equation (25)

Using the same assumptions given previously, the diffusion equation is the same as (A1). The initial condition is:

$$C\Big/_{t=o} = C_I \tag{A28}$$

C_I is the initial soda concentration in the glass. The boundary condition at x = o is given by the following:

$$\frac{\partial C}{\partial t}\Big/_{x=o} = -KAC \tag{A29}$$

The second boundary condition is a requirement that the concentration be bounded as x goes to infinity.

Assuming that the final equilibrium concentration of soda in the glass is much smaller than the initial soda concentration, we may integrate (A29) and apply (A28) to obtain the following:

$$C_{x=o} = C_I e^{-KAt} \tag{A30}$$

Expanding (A30) in a Taylor's series expansion gives:

$$C_{x=o} = C_I \left\{ 1 - KAt + \frac{(KAt)^2}{2!} \frac{(KAt)^3}{3!} + \frac{(KAt)^4}{4!} - \ldots \right\} \tag{A31}$$

If KAt is much smaller than unity, that is a small reaction rate), then an approximation to (A31) can be immediately written by throwing out all of the nonlinear terms.

$$C\Big/_{x=o} \approx C_I(1-KAt) \tag{A32}$$

Solving the diffusion equation can be made easier if we make the initial condition homogeneous. Doing this, one may obtain:

$$C' = 0 \qquad \text{at } t = 0 \tag{A33}$$

and

$$C' = C_I KAt \quad \text{at } x = o \tag{A34}$$

where:

$$C' = C_I - C \tag{A35}$$

Taking a Laplace transform of C' and substituting the initial condition (A33) gives the following result:

$$\frac{d^2g}{dx^2} - sg = 0 \tag{A36}$$

where

$$g = \mathcal{L}\left\{C'(x,t)\right\} = \int_0^\infty e^{-st} C' dt \tag{A37}$$

The general solution to (A36) is:

$$g = a_1 \exp\left(-\sqrt{\frac{s}{D}}\ x\right) + a_2 \exp\left(\sqrt{\frac{s}{d}}\ x\right) \qquad \text{(A38)}$$

However, since C' must be bounded for all x, g must therefore be bounded. This makes a_2 equal to zero, or:

$$g = a_1 \exp\left(-\sqrt{\frac{s}{d}}\ x\right) \qquad \text{(A39)}$$

One could attempt to transform (A34) and substitute the result into (A39), whereby an inverse transform may result in a solution. However, this method gives a transform that is not readily solvable. So one must use Duhamel's, or the convolution theorem to try and attain an answer.[17]

The convolution theorem, briefly stated, is as follows:

Given two functions g and h in the Laplace domain, and their corresponding functions in real space are given by G and H, respectively; the inverse of the product of g and h will be given by the following equation:

$$\mathcal{L}^{-1}\{g*h\} = \int_0^t G(\lambda)H(t-\lambda)d\lambda \qquad \text{(A36)}$$

Recasting (A39) by defining the following terms:

$$f = \exp\left(-\sqrt{\frac{s}{D}}\ x\right) \qquad \text{(A37)}$$

and by noting that:

$$a_1 = \mathcal{L}\{C_I KAt\} \qquad \text{(A38)}$$

This, with the convolution theorem gives the following result:

$$C' = \mathcal{L}^{-1}\{g\} = \mathcal{L}^{-1}\{f \cdot a_1\} = \int_0^t F(\lambda)A_1(t-\lambda)d\lambda \qquad (A39)$$

By the residue theorem:

$$F(t) = \frac{x}{2\sqrt{\pi D}}\, t^{-3/2} \exp\left(\frac{-x^2}{4Dt}\right) \qquad (A40)$$

Substitution of (A40) and (A34) into (A39) yields:

$$C' = \frac{x}{2\sqrt{\pi D}} \lambda^{-3/2} \exp\left(\frac{-x^2}{4D\lambda}\right) C_I KA(t-\lambda)d\lambda \qquad (A41)$$

on letting $v^2 = \frac{x^2}{4D\lambda}$ and rearranging:

$$C' = \frac{2C_I}{\sqrt{\pi}} \int_{\frac{x}{2\sqrt{Dt}}}^{\infty} e^{-v^2} KA\left(t - \frac{x^2}{4Dv^2}\right) dv$$

$$= \frac{2KA}{\sqrt{\pi}} \int_{\frac{x}{2\sqrt{Dt}}}^{\infty} e^{-v^2} \left(t - \frac{x^2}{4Dv^2}\right) dv \qquad (A42)$$

Integration of (A42) can be done using complex analysis. The result of the integration is:

$$C' = 4C_I KAt\, i^2\mathrm{erfc}\left(\frac{x}{2\sqrt{Dt}}\right) \qquad (A43)$$

where

$$i^2\mathrm{erfc}(\lambda) = \frac{1}{4}\left\{(1+2\lambda^2)\mathrm{erfc}(\lambda) - \frac{2}{\sqrt{\pi}}\lambda e^{-\lambda^2}\right\} \qquad (A44)$$

so:

$$C = C_I\left\{1 - 4KAti^2\mathrm{erfc}\ \frac{x}{2\sqrt{Dt}}\right\} \qquad (A45)$$

The rate of loss of soda from the glass is given by:

$$J = \left(D\frac{\partial C}{\partial x}\right)_{x=0} \qquad (A46)$$

Integrating (A46) with respect to time will given the total amount of soda lost from the glass at some time after the initiation of the reaction.

$$\frac{\partial C}{\partial x} = \frac{4C_I KAt}{2\sqrt{Dt}} \text{ ierfc}(x/2\sqrt{Dt}) \tag{A47}$$

where:

$$\text{ierfc}(\lambda) = \frac{1}{\sqrt{\pi}} e^{-\lambda^2} - \lambda \text{erfc}(\lambda) \tag{A48}$$

Solving for the flux:

$$J = \left\{ 2C_I KA \quad Dt \text{ ierfc} \left(\frac{x}{2\sqrt{Dt}} \right) \right\}_{x=o}$$

$$= 2C_I KA \sqrt{\frac{Dt}{\pi}} \tag{A49}$$

Integrating (A49) with respect to t:

$$\frac{N}{A} = \frac{4}{3} C_I KA \sqrt{\frac{D}{\pi}} t^{3/2} \tag{A50}$$

By stoichiometry:

$$\frac{N_{(\text{sodium})}}{A} = \frac{8}{3} C_I KA \sqrt{\frac{D}{\pi}} t^{3/2} \tag{A51}$$

Also:

$$M_t = M_w(\text{Na}) \, N_{(\text{sodium})}$$

and

$$C_I = \frac{\rho}{M_{W(\text{glass})}}$$

Since M_t in the experiment is measured in terms of milligrams, we must multiply the resulting solution by 1000.

The final result is:

$$\frac{M_t}{A} = \frac{8000}{3} \frac{\rho K A \sqrt{D}\, M_w(Na)}{M_{w(glass)}\, \sqrt{\pi}}\, t^{3/2} \qquad (A52)$$

List of Figures Used in this Study

Fig. 1. The experimental geometry used for the glass coating on the metal.

Fig. 2. The experimental apparatus used in the weight loss experiments.

Fig. 3. The normalized sodium weight loss at various temperatures.

Fig. 4. FeO doped sodium disilicate glass reaction profiles on two different substrates.

Fig. 5. Sodium weight loss data plotted as 1st order kinetics (see text for full description).

Fig. 6. Sodium weight loss data plotted as 1st order kinetics, with the ordinate expanded and for lower temperatures.

Fig. 7a. Sodium weight loss data plotted for various temperatures assuming a diffusion limiting process to occur.

Fig. 7b. The same as 7a., only the scale is expanded for clarity.

Fig. 8. Sodium weight loss data linearized on a log-log plot for short time (less than 60 to 90 minutes).

Fig. 9. A comparison of the raw data to the theoretical results predicted by equation (24).

Fig. 10. The Iron(II) oxide, soda, silica phase diagram, illustrating the reaction path taken by the Iron-Sodium Disilicate reaction system.

Fig. 11. An SEM photograph showing the silica rich precipitates forming within the glass after two hours of reaction at 1000°C.

Fig. 12. The Arrehnius plot of the interface reactions occurring between 955 and 1145°C, for the Iron-sodium disilicate system.

Fig. 13. A plot of the reaction profiles, showing the differences in reactivity between aged and as received Marz-A iron specimens with sodium disilicate glass.

Fig. 14. A plot of the reaction profiles demonstrating the differences in reactivity between Armco iron and as received Marz-A iron specimens with sodium disilicate glass.

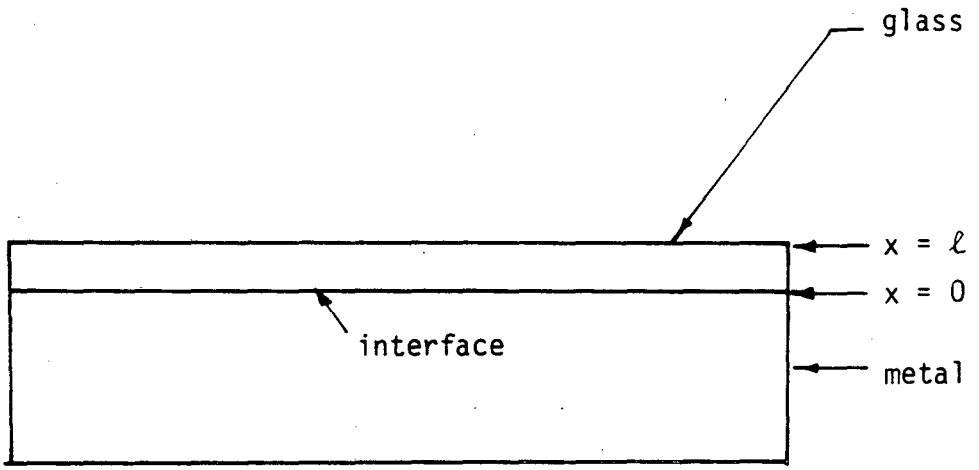

XBL 832-8486

Figure 1.

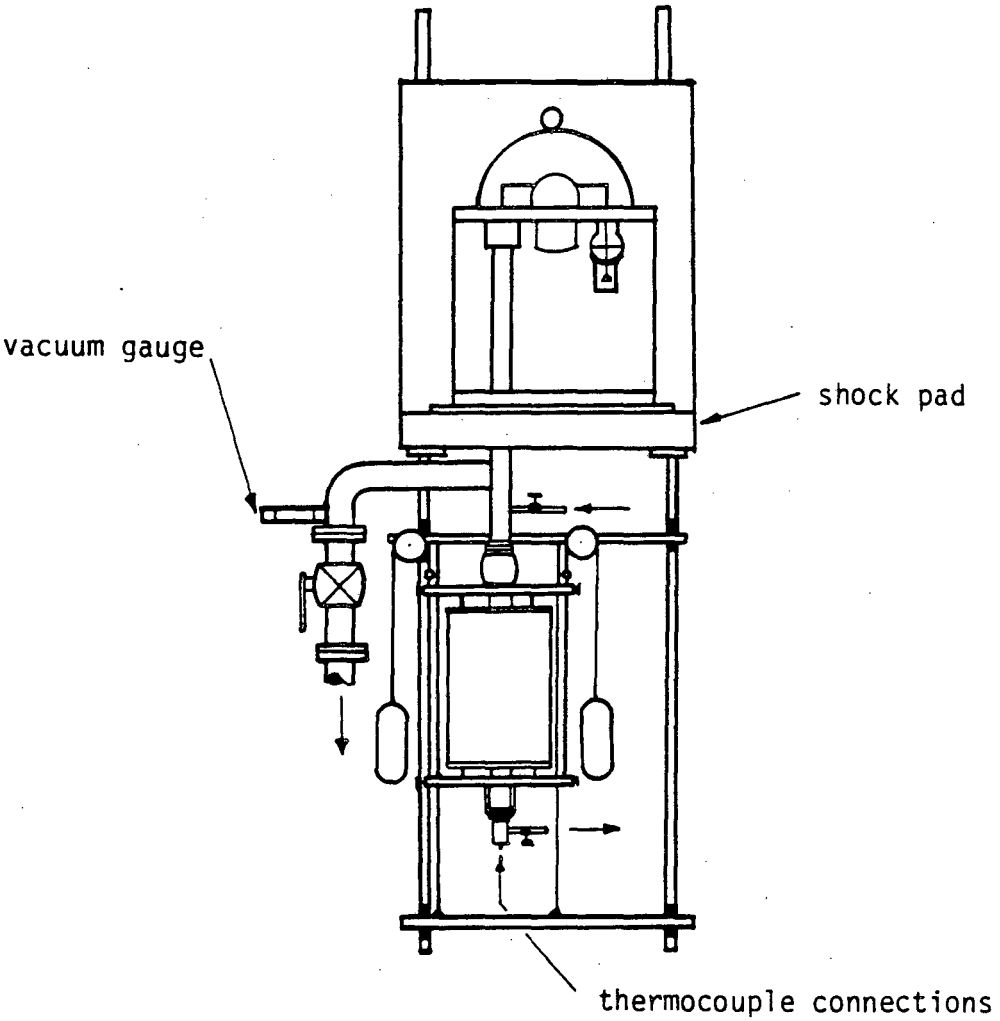

XBL 832-8487

Figure 2.

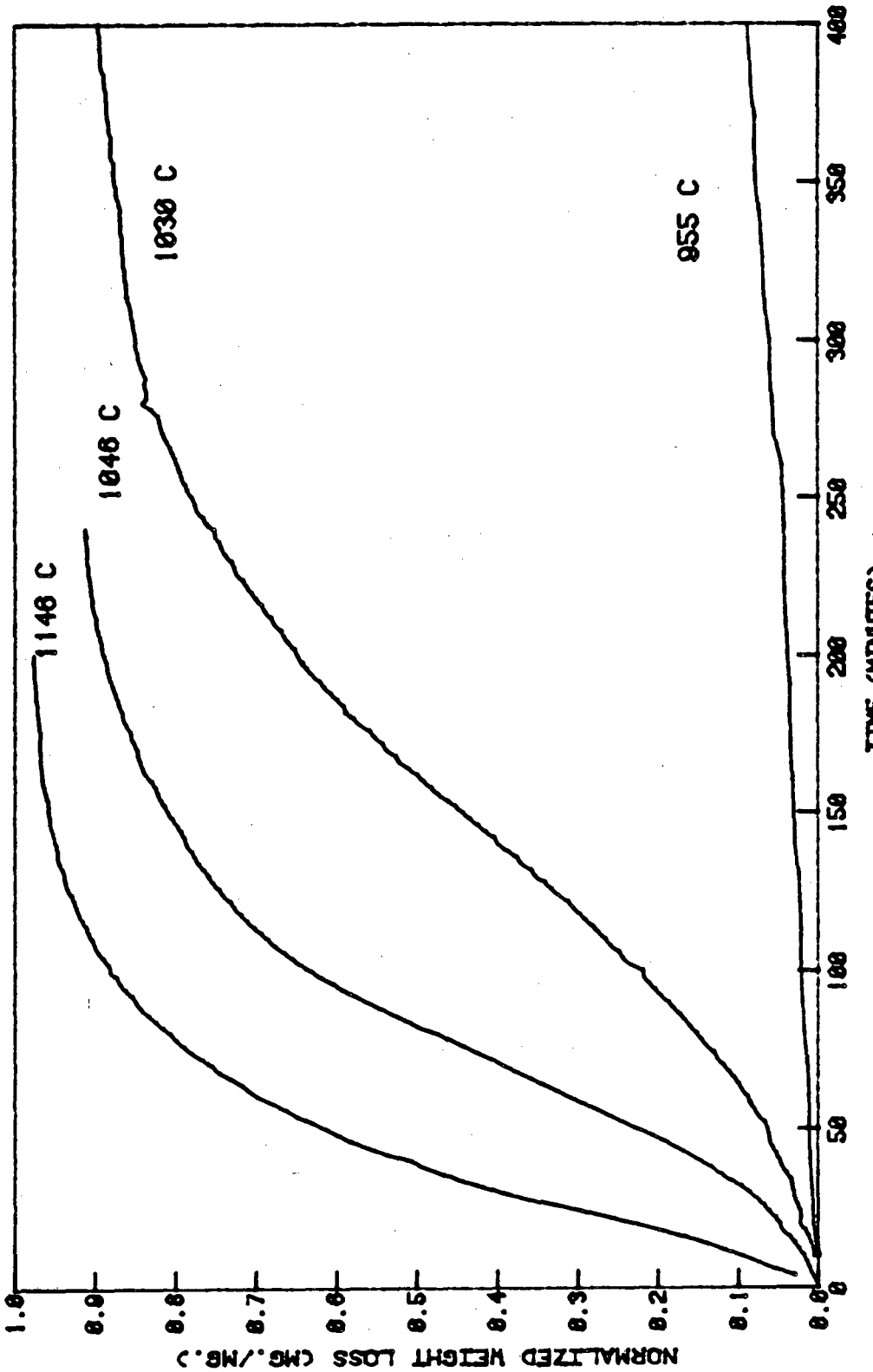

XBL 832-8488

Figure 3.

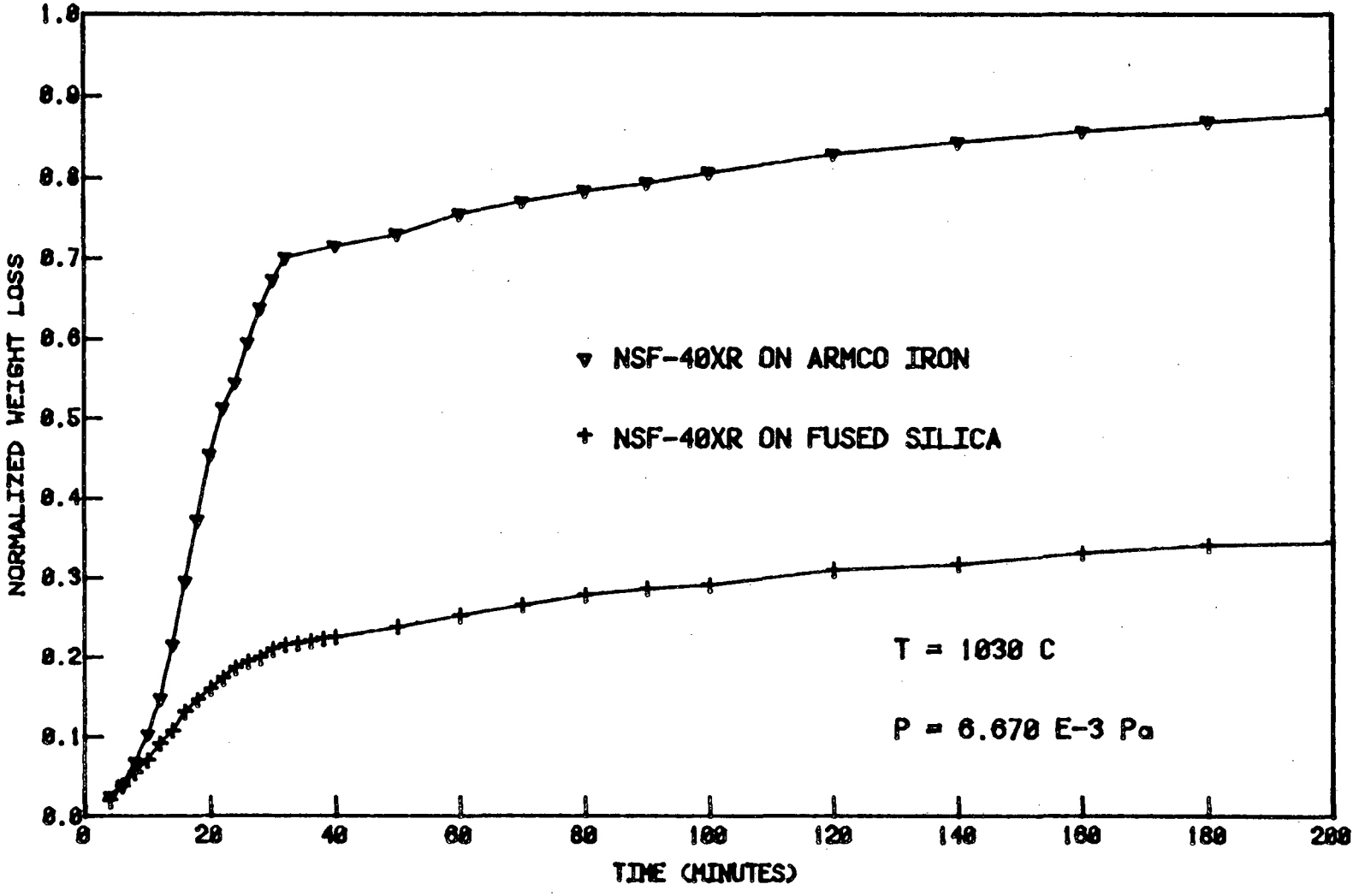

Figure 4.

XBL 832-8489

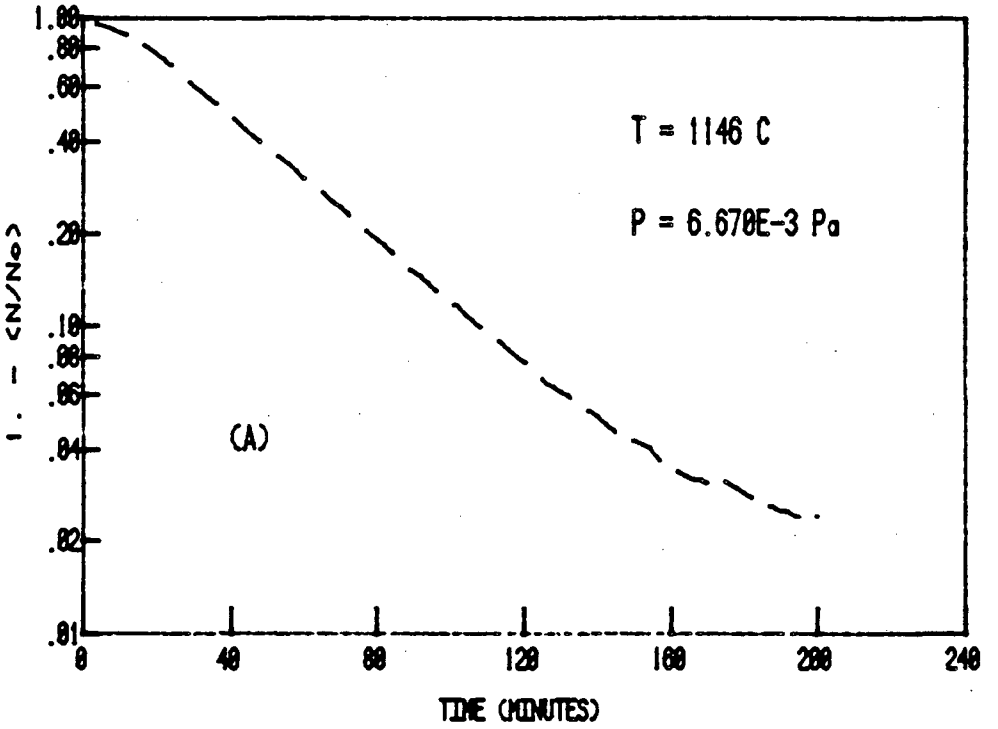

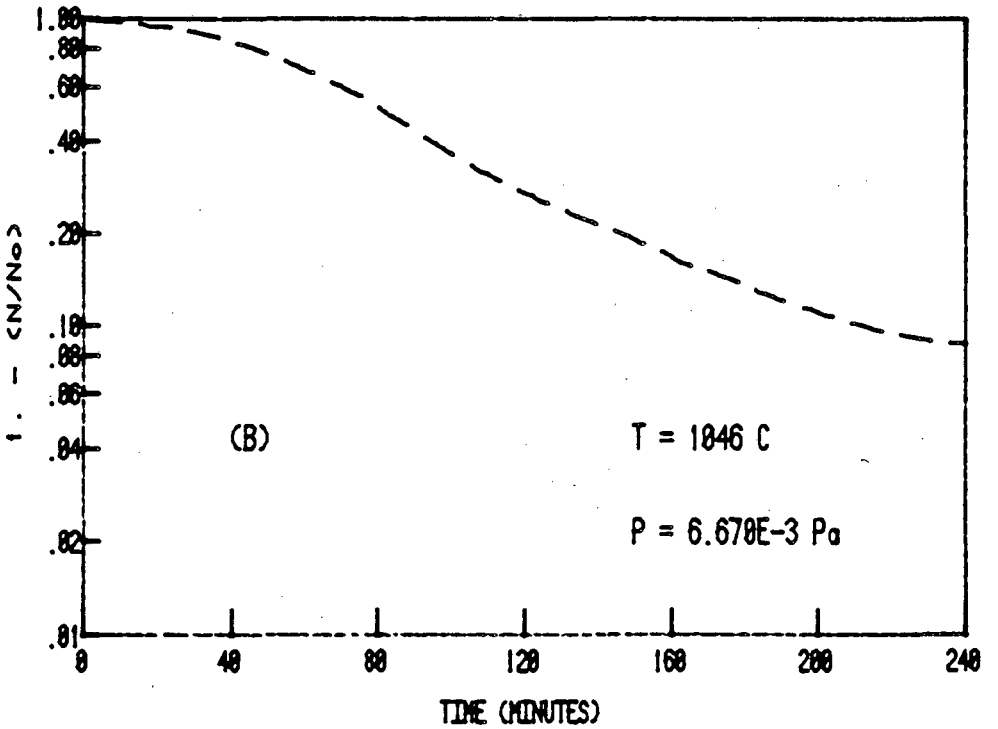

Figure 5.

XBL 832-8491

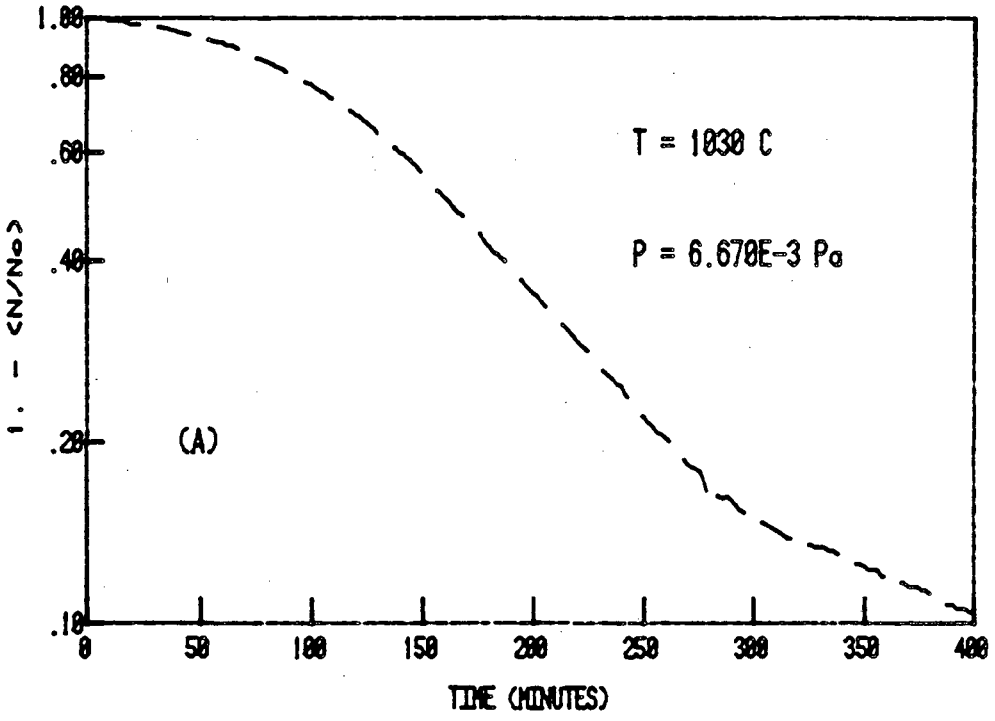

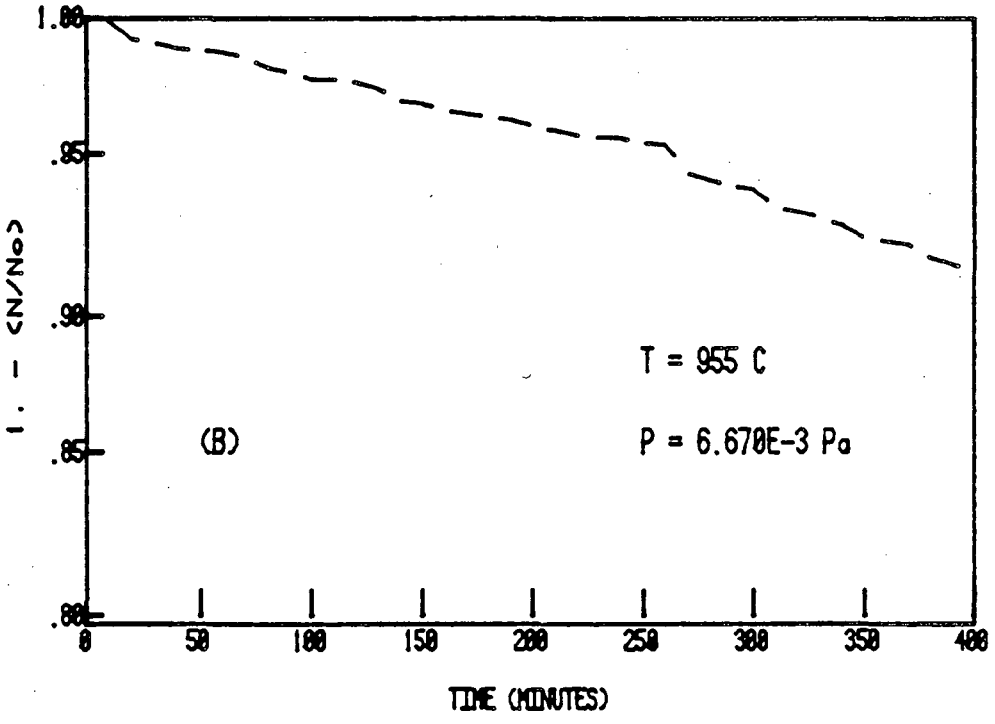

XBL 832-8490

Figure 6.

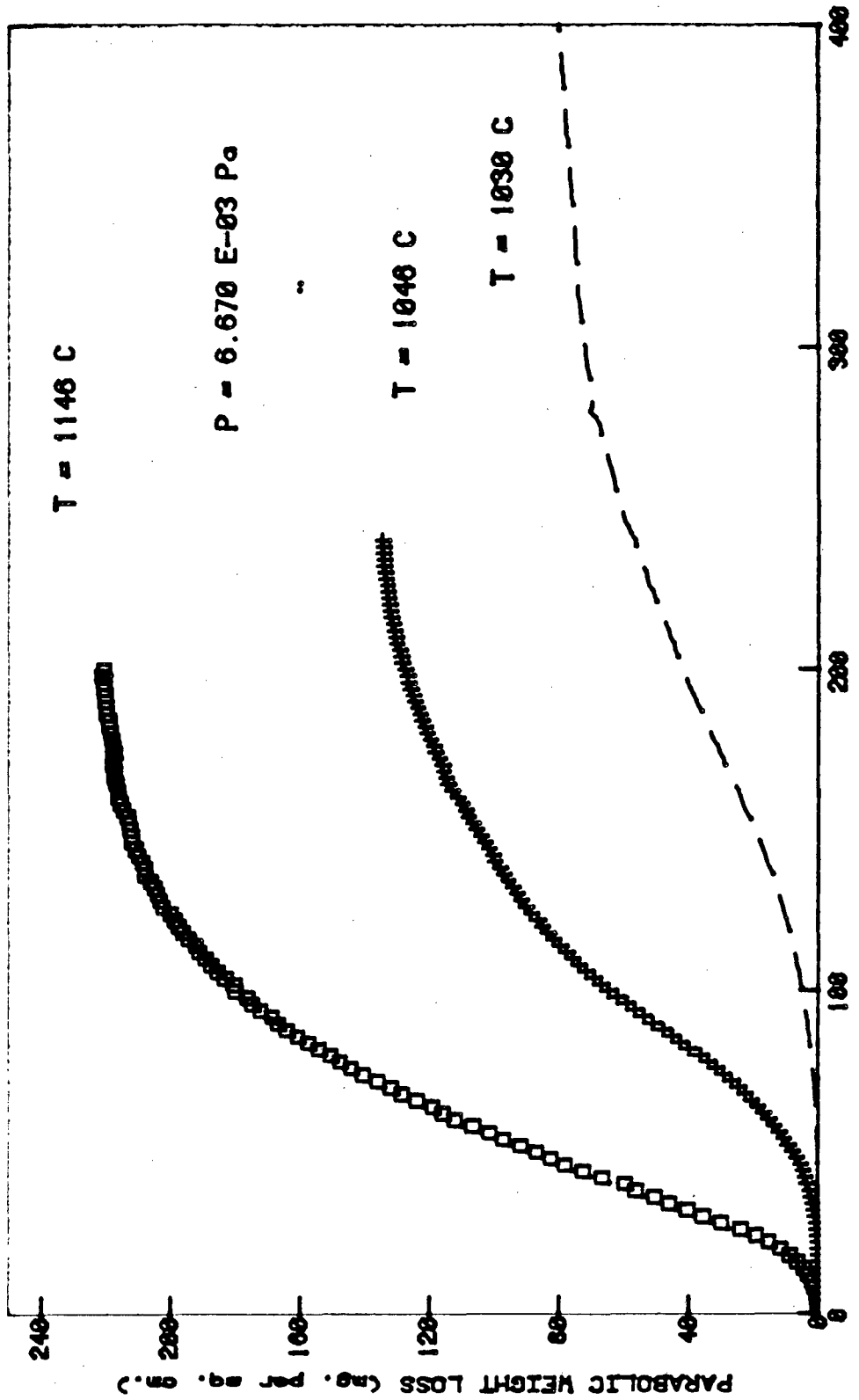

XBL 832-8492

Figure 7A.

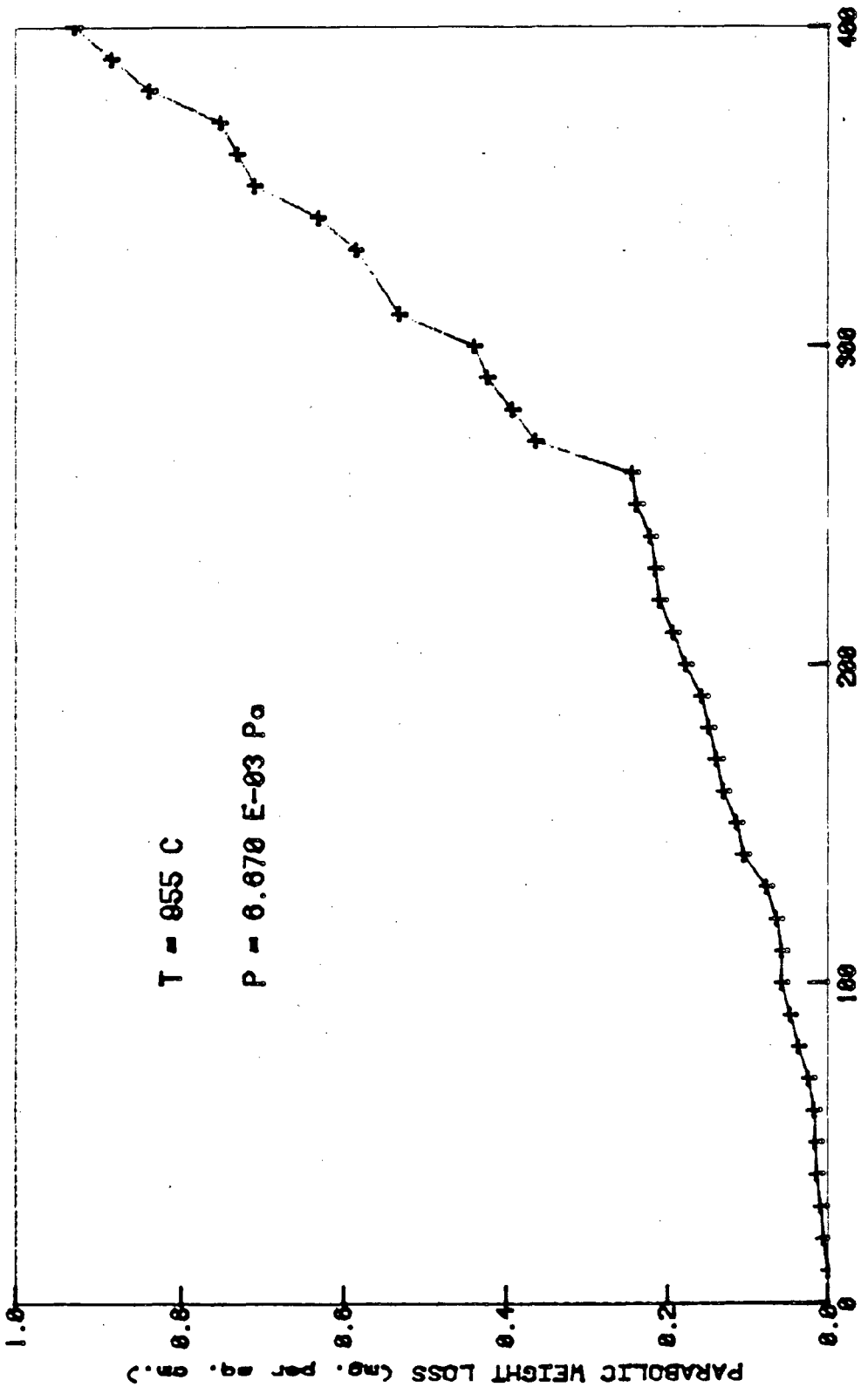

XBL 832-8493

Figure 7B.

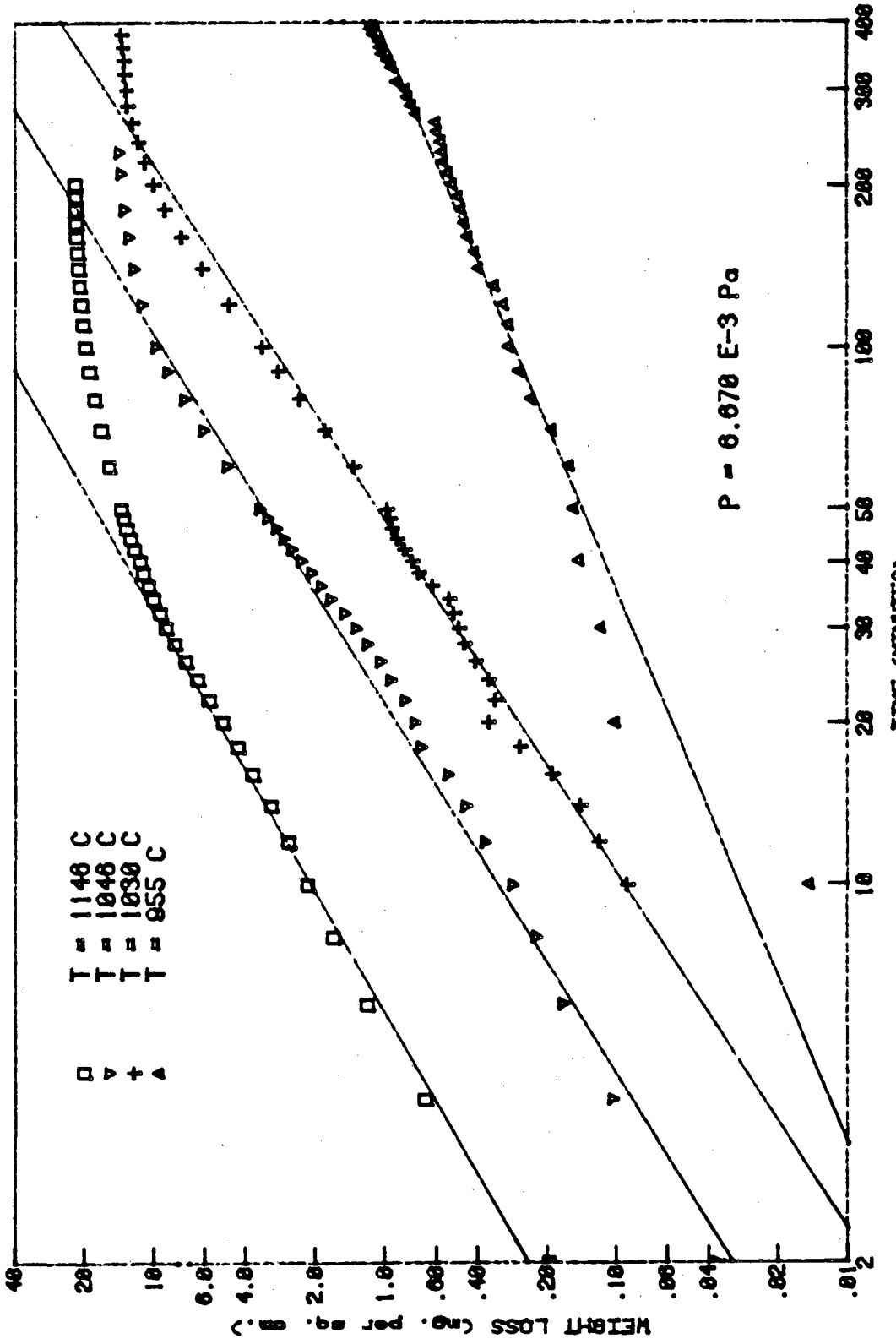

XBL 832-8494

Figure 8.

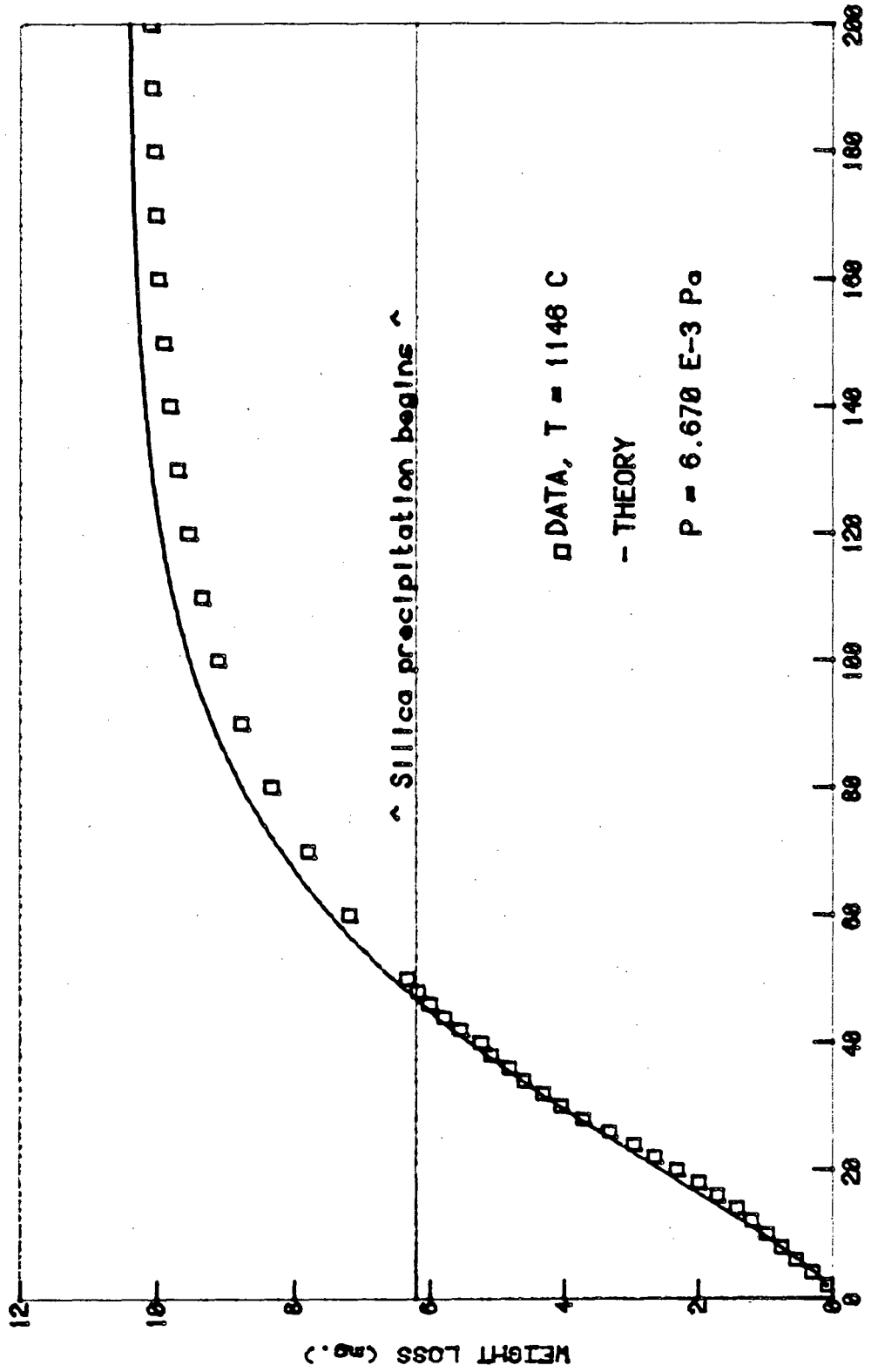

XBL 832-8495

Figure 9.

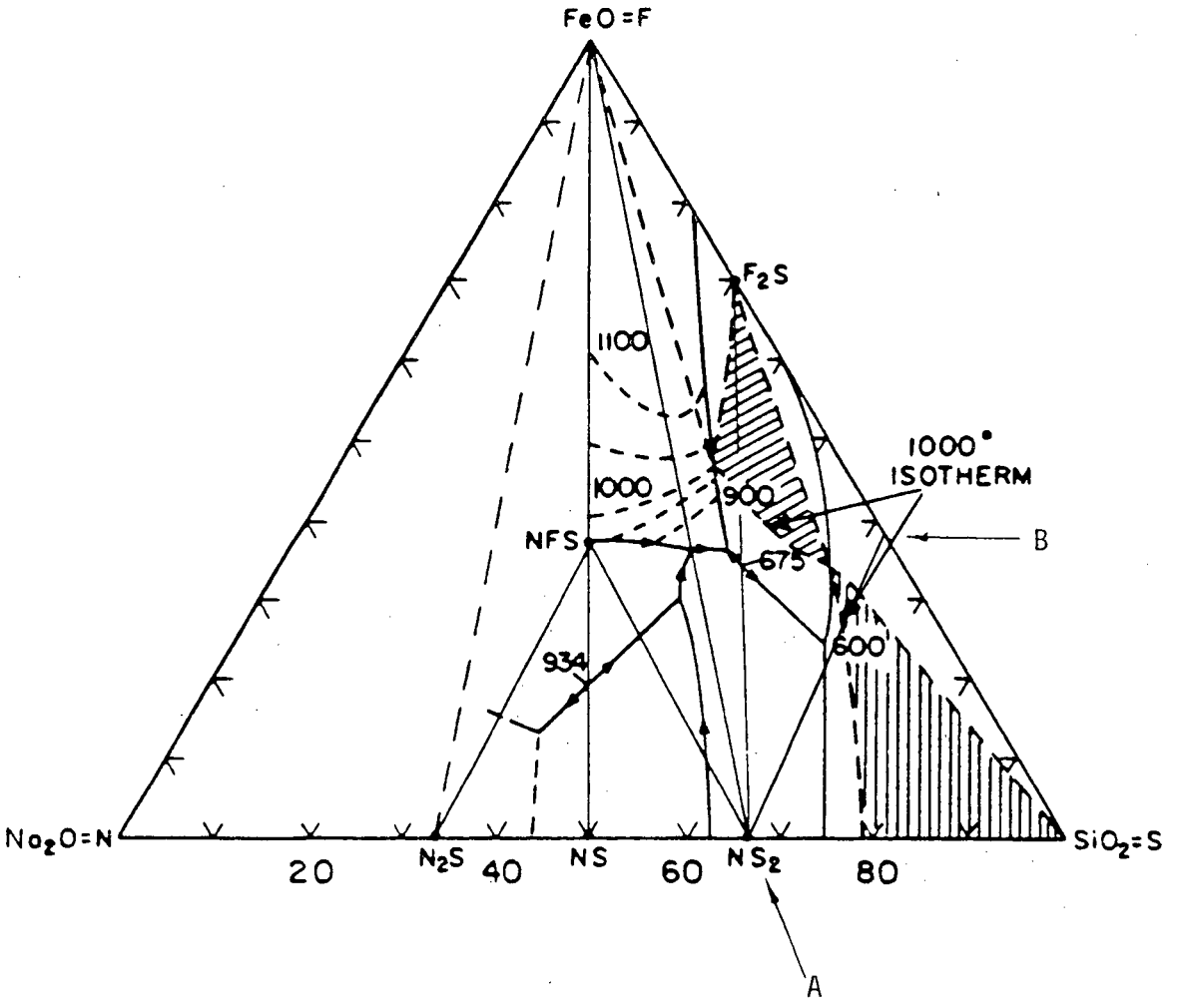

XBL 697-867A

Figure 10.

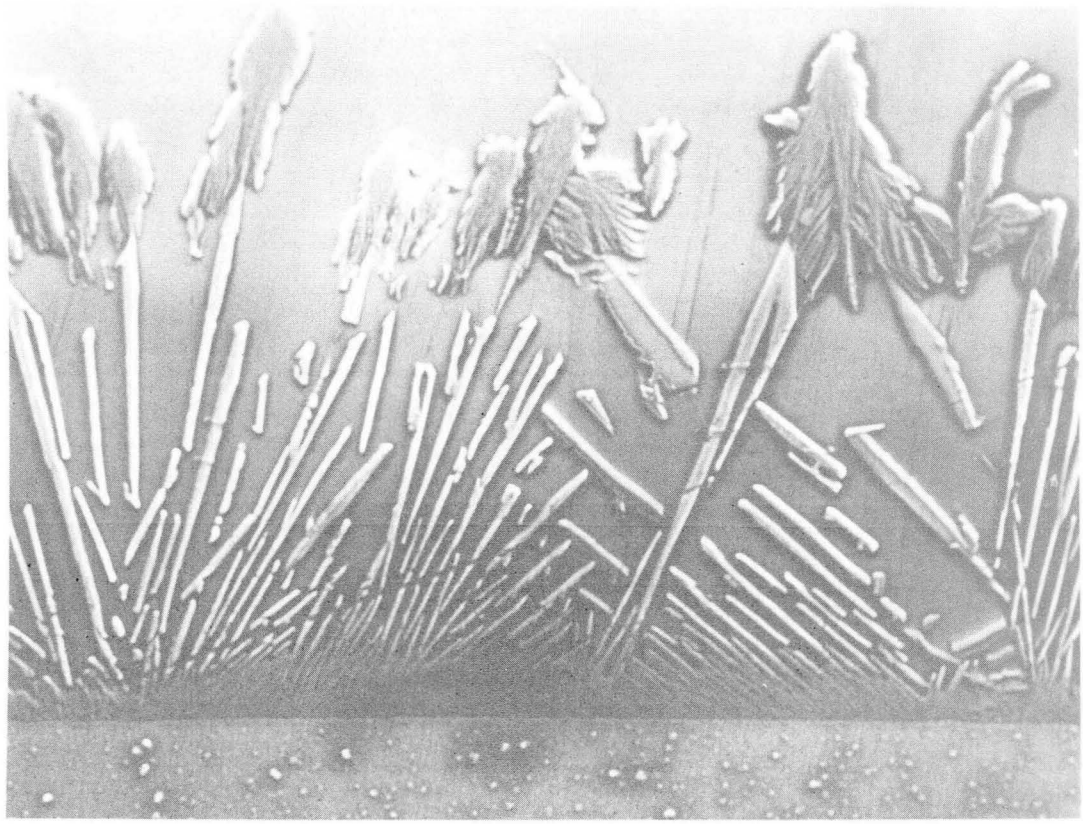

XBB 790-13663

Figure 11.

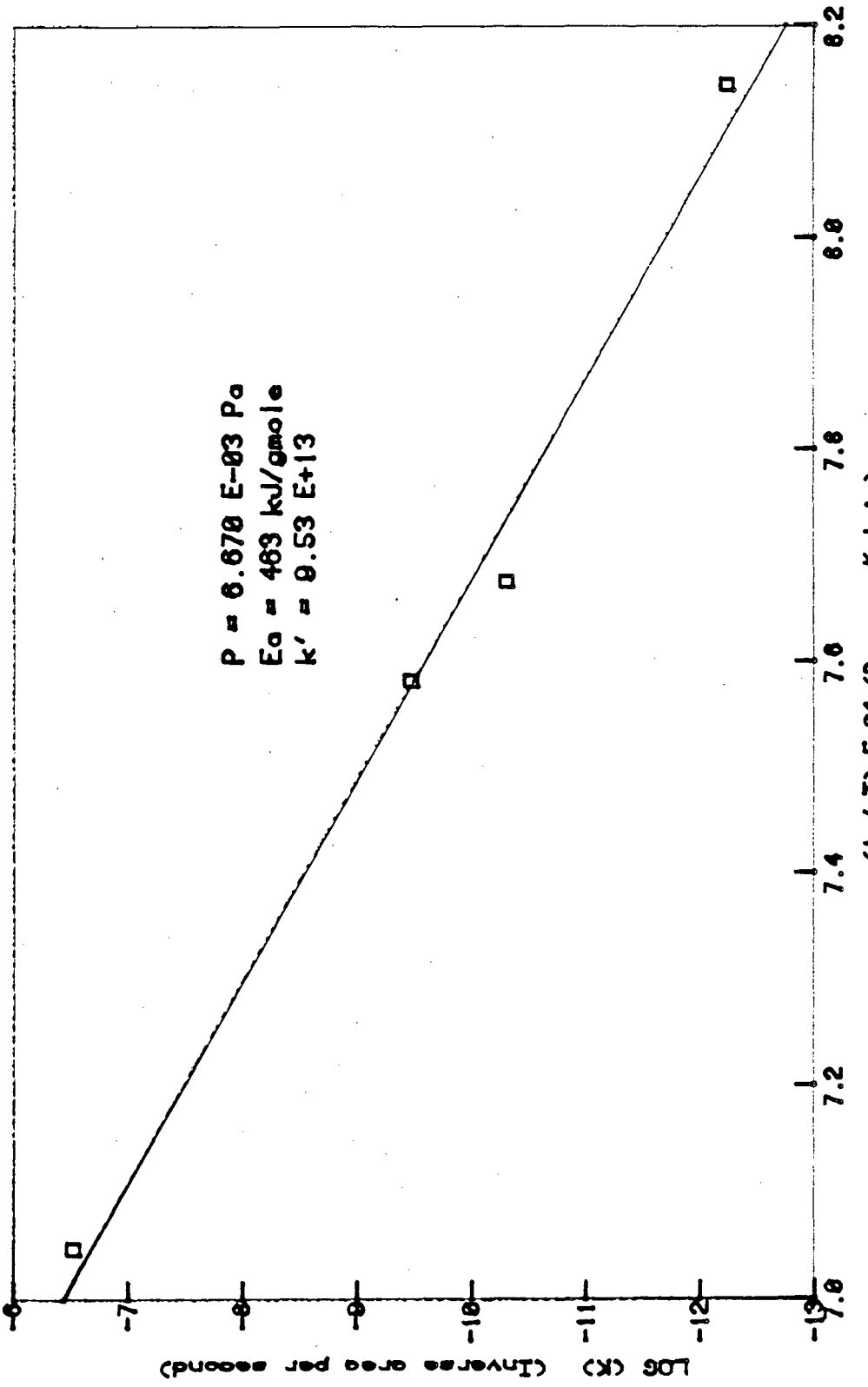

XBL 832-8496

Figure 12.

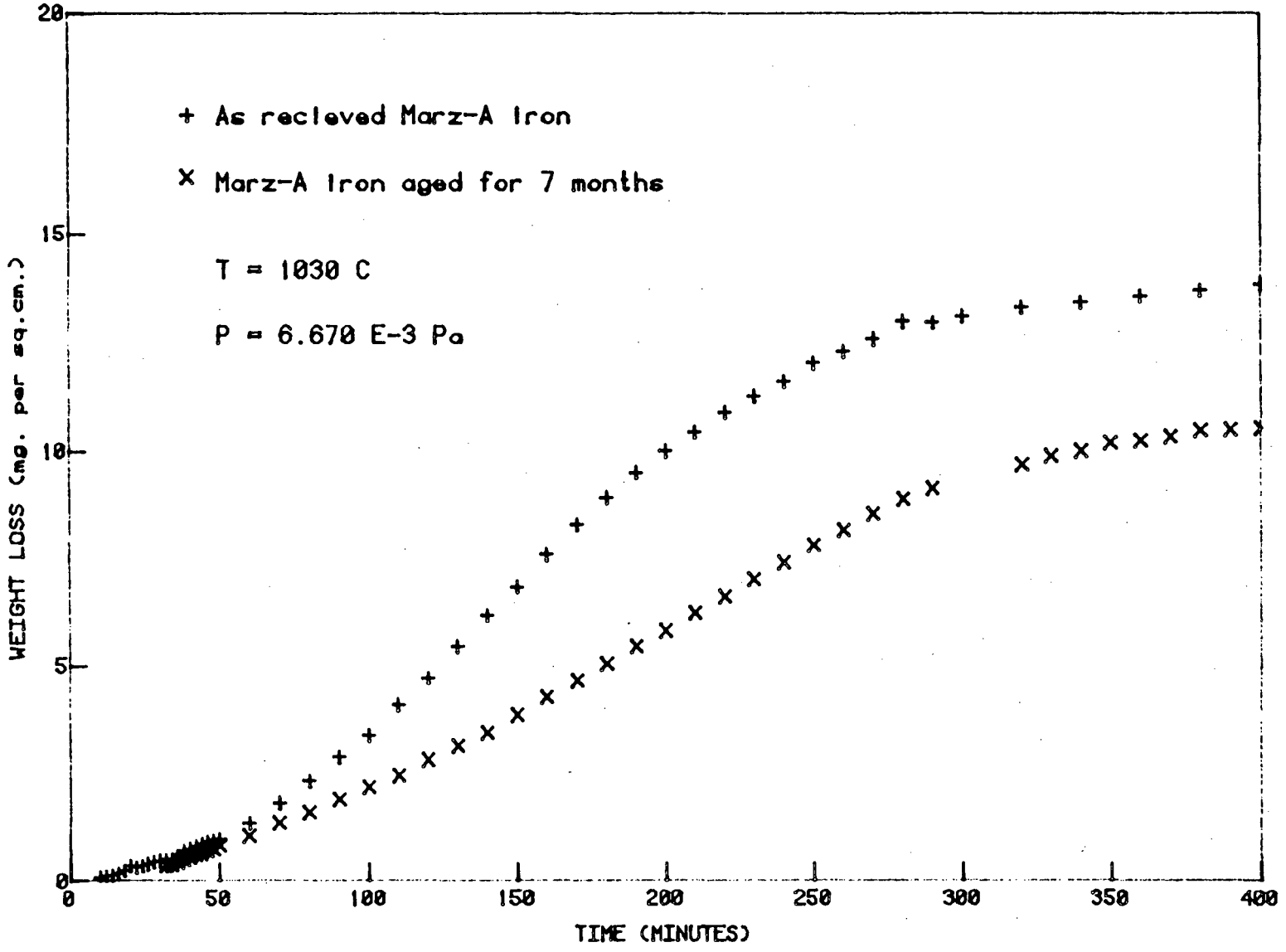

Figure 13.

XBL 832-8497

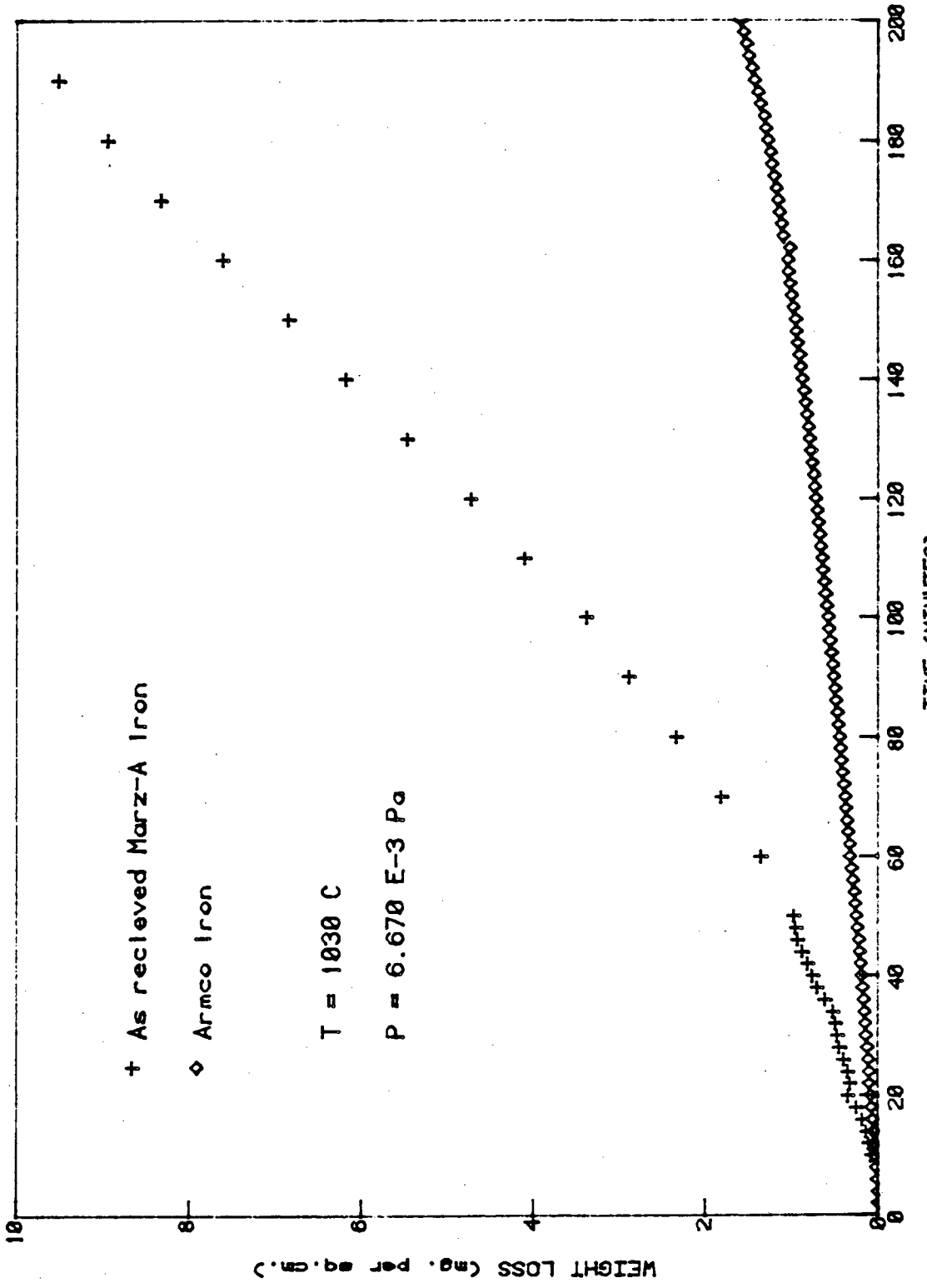

XBL 832-8498

Figure 14.

TECHNICAL INFORMATION DEPARTMENT
LAWRENCE BERKELEY LABORATORY
UNIVERSITY OF CALIFORNIA
BERKELEY, CALIFORNIA 94720